Early View publication on www.interscience.wiley.com
(issue and page numbers not yet assigned;
citable using Digital Object Identifier – **DOI**)

Laser Phys. Lett., 1–5 (2010) / **DOI** 10.1002/lapl.201010067

Laser Physics Letters

Abstract: We demonstrate passive mode-locking of a Bi-doped fiber laser using a nanotube-based saturable absorber. We achieve stable mode-locking in both the all-normal and net anomalous dispersion regimes. Near transform-limited 4.7 ps solitons are generated in the average-soliton regime, with a chirped fiber Bragg grating used for dispersion compensation to retain an all-fiber format.

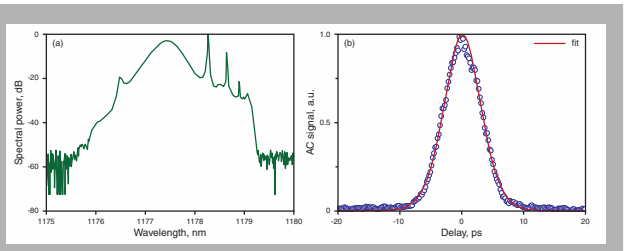

(a) – optical spectrum of Bi-doped soliton fiber laser and (b) – corresponding autocorrelation function

Bismuth fiber integrated laser mode-locked by carbon nanotubes

E.J.R. Kelleher, [1,*] *J.C. Travers,* [1] *Z. Sun,* [2] *A.C. Ferrari,* [2] *K.M. Golant,* [3] *S.V. Popov,* [1] *and J.R. Taylor* [1]

[1] Femtosecond Optics Group, Physics Department, Prince Consort Road, Imperial College, London SW7 2AZ, UK
[2] Department of Engineering, University of Cambridge, Cambridge CB3 0FA, UK
[3] V.A. Kotel'nikov Institute of Radio Engineering and Electronics, 11-7, Mokhovaya Str., Moscow 125009, Russia

Received: 1 July 2010, Revised: 20 July 2010, Accepted: 23 July 2010
Published online: XX Xxxxxxx 2010

Key words: mode-locked lasers; fiber lasers; nanomaterials

1. Introduction

Bismuth doping of silica glass fiber has recently emerged as a potentially useful fiber-based technology because it provides gain in a region of the near-infrared inaccessible to rare-earth-doped fibers, such as Yb and Er [1–3]. A broad emission band (1100–1250 nm) makes Bi-doped fiber attractive for the generation of short pulses. Recently, it was shown that the luminescence band could be further extended, as far as 1550 nm, with modification of the core glass composition and optimization of the pump wavelength [4,5]. Bi-doped fiber systems mode-locked using semiconductor saturable absorber mirrors (SESAMs) have been reported [6–8]. However, SESAMs are typically complex and expensive quantum well devices. While other all-fiber passive mode-locking schemes are available [9,10], adopting an artificial saturable absorber approach can result in poor self-starting operation. Nanotube and graphene-based saturable absorbers have recently emerged as a competitive alternative to SESAMs and have been used to mode-lock a number of rare-earth-doped fiber lasers due to their outstanding properties, such as subpicosecond recovery time, broad operation range, polarization insensitivity, easy fabrication, and environmental robustness [11–28].

Here, we report the use of a single-wall nanotube-based saturable absorber (SWNT-SA) to mode-lock a Bi-doped fiber ring laser. In Bi-doped lasers the cavity dispersion at the wavelength of operation is inherently normal. Hence, dispersion compensation is needed to achieve soliton-like operation, providing near transform-limited pulses. However, all-normal dispersion (ANDi) lasers can support stable dissipative soliton solutions, carrying a large linear chirp [29], providing a source of high-energy ultrafast pulses [30,31]. Their pulse-dynamics has received significant attention [29,32,33]. We show that our Bi-doped fiber laser operates with contrasting dispersion maps producing both 558 ps pulses and near-transform limited 4.7 ps pulses in the ANDi and average-soliton regime, respectively. In the average-soliton regime dispersion compensation is provided by a chirped fiber Bragg grating (CFBG) to retain an all-fiber format.

* Corresponding author: e-mail: ek408@ic.ac.uk

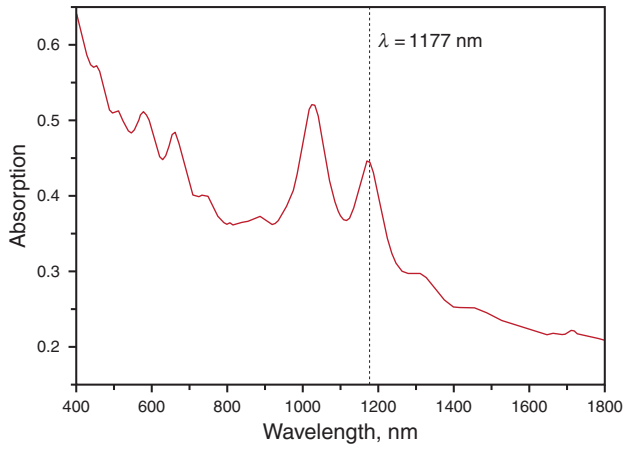

Figure 1 (online color at www.lphys.org) SWNT-SA absorption. The operation wavelength is indicated

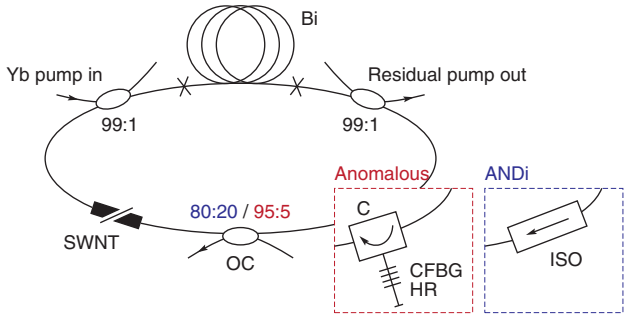

Figure 2 (online color at www.lphys.org) Experimental setup. Bi – Bi-doped fiber, OC – output coupler (with coupling ratios indicated), SWNT-SA – nanotube-based saturable absorber. Insets: C – circulator, CFBG HR – chirped fiber Bragg grating high reflector (anomalous cavity), ISO – inline optical isolator (ANDi cavity)

The band-gap of the SWNTs determines the SA operation wavelength [11,17]. This can be controlled in several ways, for example by changing the growth methods and conditions [11]. Here, we optimize our SWNT-SA for the intended operation wavelength of ∼ 1170 nm, corresponding to the peak gain of our Bi-doped fiber. To match this wavelength, we need to use SWNTs with ∼0.9 nm diameter [34]. Therefore, we select CoMoCaT SWNTs to fabricate a SWNT-polyvinyl Alcohol composite, as described in [11] and references therein. The absorption spectrum of the composite is shown in Fig. 1. A strong peak is observed at ∼ 1170 nm, close to the desired operation wavelength, in correspondence to the first transition of (7,6) SWNTs [34]. Another band at ∼ 1028 nm is also seen, assigned to (6,5) SWNTs [34].

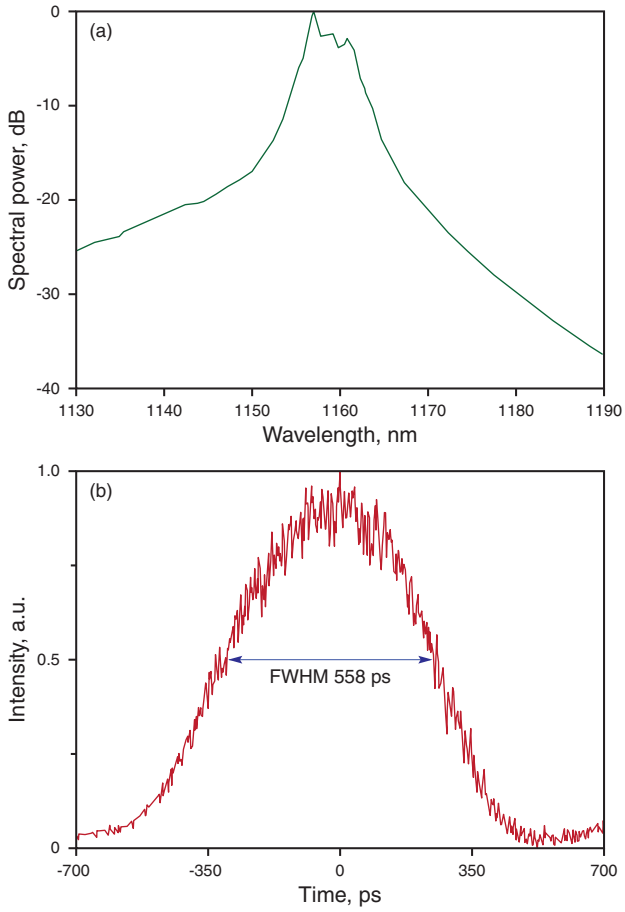

Figure 3 (online color at www.lphys.org) (a) – optical spectrum of the ANDi laser, (b) – corresponding temporal pulse shape

2. Experimental setup

The all-fiber geometries are shown schematically in Fig. 2. We investigated two cavity configurations with contrasting dispersion maps: an ANDi cavity, because of the natural normal dispersion of the Bi-doped fiber at the wavelength of operation, and an anomalous cavity including dispersion compensation provided by a CFBG for a net anomalous dispersion. Common to both configurations were a 30 m Bi-doped active fiber, core-pumped through a custom wavelength division multiplexer (WDM) using a commercial 10 W Yb-doped fiber laser, a fused fiber output coupler, and the SWNT-SA. The residual pump light was coupled out of the cavity with a second WDM. The alumosilicate-core Bi-doped fiber preform was fabricated using a surface plasma chemical vapor deposition (SPCVD) process [35] and drawn into a single-mode fiber compatible with commercial Corning HI-1060 to facilitate direct fusion splicing to passive cavity components with low loss: typically less than 0.1 dB. Such a long length of active fiber is needed because of low pump absorption

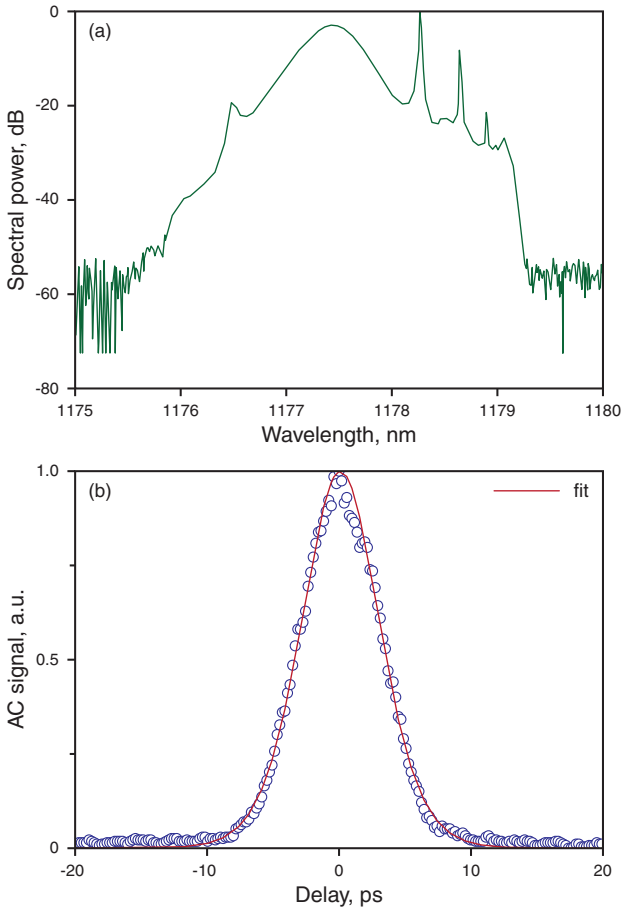

Figure 4 (online color at www.lphys.org) (a) – optical spectrum of the dispersion compensated anomalously dispersive cavity, with prominent solitonic sides bands. (b) – intensity autocorrelation, with sech^2 fit in red

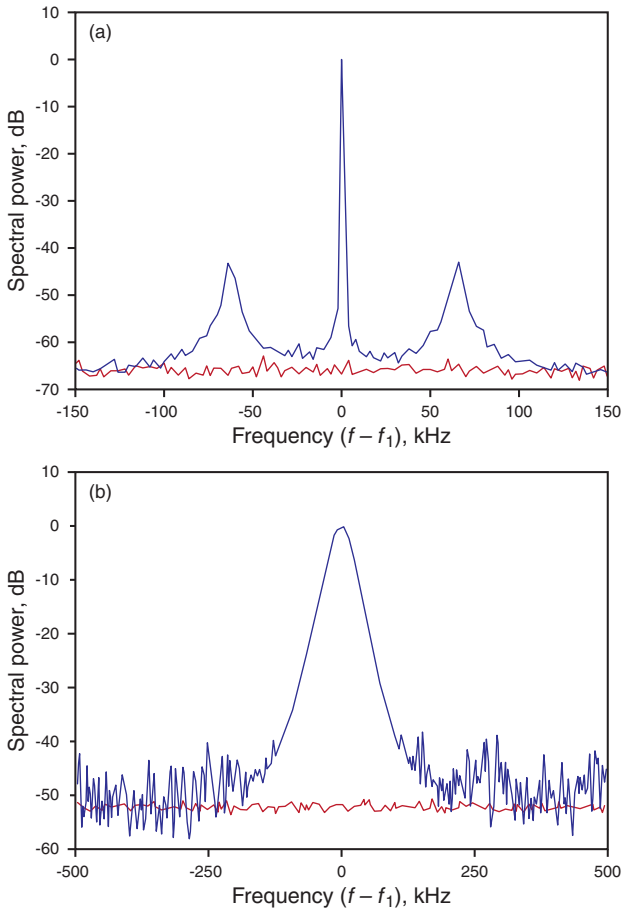

Figure 5 (online color at www.lphys.org) Electrical spectra of the fundamental harmonic (f_1). (a) – ANDi cavity, (b) – anomalous cavity. The radio frequency background is shown with a red line

and a relatively low gain coefficient [7,36]. The gain had a strong temperature dependence, being enhanced when the Bi-doped fiber was cooled to 77K, which we did for all experiments. The SWNT-SA film was integrated using two APC fiber connectors, having typically 3.5 dB insertion loss, with 2 dB attributed to the linear transmission of the composite (Fig. 1). Unidirectionality was imposed upon both cavities with the inclusion of an inline fiber-pigtailed isolator in the ANDi oscillator and a fiber-pigtailed optical circulator in the net anomalous case. A 20% output coupler was used in the ANDi laser to maximize the output pulse energy. The output coupling ratio was modified (to 5%) to facilitate mode-locking in the average-soliton regime, where the roundtrip loss was greater because of the addition elements providing dispersion compensation.

3. Results and discussion

Self-starting, fundamental continuous-wave (CW) mode-locking was achieved in both cavity configurations, with a $\sim$5 MHz repetition rate defined by the long cavity ($\sim$40 m). The mode-locking threshold was considerably higher in the ANDi laser, with stable CW mode-locking obtained for $\sim$1.5 W pump power. At reduced pump power strong Q-switched mode-locking was dominant. Stable, pure Q-switch pulses were obtained for increased pumping, itself a useful regime of operation for some applications [37]. The ANDi laser generated 558 ps pulses with a minimum 3 dB bandwidth of 3.3 nm centered at 1157 nm (Fig. 3a), giving a time-bandwidth product of $\sim$412 indicative of a large chirp, and a pulse energy of 1.4 nJ, assuming most of the power to be contained within the spectral profile of the pulse. The temporal pulse shape, measured using a photodiode with a 15 ps rise time and a 50 GHz sampling oscilloscope, is shown in Fig. 3b.

In the dispersion compensated net anomalous cavity, with the inclusion of the circulator and CFBG, we obtained average-soliton operation. The average output power was considerably lower in the net-anomalous case, typically 10 – 15 μW for 200 mW pumping, with modest pulse en-

ergies ~ 3 pJ. Fig. 4a shows the output spectrum centered at 1177 nm, defined by the passband of the CFBG, with prominent soliton sidebands and a full width half maximum (FWHM) bandwidth of 0.35 nm. The spikes on the long-wavelength edge can be attributed to high-order dispersion due to the CFBG. Fig. 4b is the corresponding intensity autocorrelation trace, fitted with the autocorrelation shape expected for a sech^2 pulse. The pulse duration was 4.7 ps, giving a time-bandwidth product of 0.36, near transform-limited for a sech^2. The achieved pulse width is limited by the intracavity dispersion. Sub-picosecond pulses should be obtainable with more balanced dispersion compensation. Although reliable CW mode-locking was achieved for a fixed pump power, because of the low gain coefficient of the active fiber and relatively high modulation depth of the SWNT-SA ($\sim 12\%$ at 1.064 μm) the system would become unstable with elements of Q-switching for increased pump power.

The radio frequency (RF) spectra of the fundamental mode-locking harmonic for the two operation regimes are shown in Fig. 5. Prominent side bands, characteristic of Q-switching instabilities and high intensity noise, appear in Fig. 5a at a resolution bandwidth of 300 Hz. Observations of the pulse-train on a 400 MHz analog oscilloscope supported the existence of temporal fluctuations over longer time-scales. The peak to pedestal extinction of the fundamental harmonic in the RF spectrum of the anomalous cavity (Fig. 5b) is at least 50 dB at the resolution limit of the device (30 Hz), limited by the noise floor of the RF analyzer. The linewidths in both regimes are again device limited, indicating low temporal inter-pulse jitter. Measurement of the pulse train on a 400 MHz analog oscilloscope confirmed stable CW mode-locking in the anomalous regime, with no signs of transient effects nor Q-switching.

4. Conclusions

We demonstrated a Bi-doped fiber laser mode-locked with a nanotube-based saturable absorber. Stable, self-starting fundamental mode-locking was achieved in an ANDi cavity, producing 558 ps pulses, with pulse energies up to 1.6 nJ at a 5.47 MHz repetition rate. Dispersion compensation was provided by a fiber pigtailed optical circulator and CFBG to obtain a soliton laser generating 4.7 ps near transform-limited pulses at 5.13 MHz. With more balanced dispersion compensation, for example using a suitable photonic crystal fiber, sub-picosecond pulses should be achievable, while retaining the flexibility of a compact all-fiber format.

Acknowledgements The Femtosecond Optics Group is supported by the EPSRC and the Royal Society. SVP is a Royal Society Industry Fellow, JRT and ACF are Royal Society Wolfson Research Merit Award holders. ACF acknowledges funding from the Royal Society Brian Mercer Award for Innovation, ERC grant NANOPOTS and EPSRC grant EP/GO30480/1.

References

[1] V.V. Dvoyrin, V.M. Mashinsky, E.M. Dianov, A.A. Umnikov, M.V. Yashkov, and A.N. Guryanov, in: 31st European Conference on Optical Communications, Glasgow, UK, September 25–29, 2005 (ECOC 2005), Vol. 4, p. 949.
[2] E.M. Dianov, A.V. Shubin, M.A. Melkumov, O.I. Medvedkov, and I.A. Bufetov, J. Opt. Soc. Am. B **24**, 1749 (2007).
[3] I. Razdobreev, L. Bigot, V. Pureur, A. Favre, G. Bouwmans, and M. Douay, Appl. Phys. Lett. **90**, 031103 (2007).
[4] I.A. Bufetov and E.M. Dianov, Laser Phys. Lett. **6**, 487 (2009).
[5] S.V. Firstov, I.A. Bufetov, V.F. Khopin, A.V. Shubin, A.M. Smirnov, L.D. Iskhakova, A.N. Guryanov, and E.M. Dianov, Laser Phys. Lett. **6**, 665 (2009).
[6] E.M. Dianov, A.A. Krylov, V.V. Dvoyrin, V.M. Mashinsky, P.G. Kryukov, O.G. Okhotnikov, and M. Guina, J. Opt. Soc. Am. B **24**, 1807 (2007).
[7] S. Kivisto, R. Gumenyuk, J. Puustinen, M. Guina, E.M. Dianov, and O.G. Okhotnikov, IEEE Photon. Technol. Lett. **21**, 599 (2009).
[8] S. Kivistö, J. Puustinen, M. Guina, R. Herda, S. Marcinkevicius, E.M. Dianov, and O.G. Okhotnikov, Opt. Express **18**, 1041 (2010).
[9] Z.X. Zhang, Z.Q. Ye, M.H. Sang, and Y.Y. Nie, Laser Phys. Lett. **5**, 364 (2008).
[10] B. Ibarra-Escamilla, O. Pottiez, E.A. Kuzin, R. Grajales-Coutiño, and J.W. Haus, Laser Phys. **18**, 914 (2008).
[11] T. Hasan, Z.P. Sun, F.Q. Wang, F. Bonaccorso, P.H. Tan, A.G. Rozhin, and A.C. Ferrari, Adv. Mater. **21**, 3874 (2009).
[12] S. Set, H. Yaguchi, Y. Tanaka, M. Jablonski, Y. Sakakibara, A.G. Rozhin, M. Tokumoto, M. Kataura, Y. Achiba, and K. Kikuchi, in: Optical Fiber Communications Conference, Atlanta, GA, USA, March 23–28, 2003 (OFC 2003), paper PD44.
[13] Y.-W. Song, S.Y. Set, S. Yamashita, C.S. Goh, and T. Kotake, IEEE Photon. Technol. Lett. **17**, 1623 (2005).
[14] A.G. Rozhin, V. Scardaci, F. Wang, F. Hennrich, I.H. White, W.I. Milne, and A.C. Ferrari, Phys. Stat. Sol. b **243**, 3551 (2006).
[15] J.W. Nicholson, R.S. Windeler, and D.J. DiGiovanni, Opt. Express **15**, 9176 (2007).
[16] K. Kieu and F.W. Wise, Opt. Express **16**, 11453 (2008).
[17] F. Wang, A.G. Rozhin, V. Scardaci, Z. Sun, F. Hennrich, I.H. White, W.I. Milne, and A.C. Ferrari, Nat. Nanotechnol. **3**, 738 (2008).
[18] Z.P. Sun, T. Hasan, F.Q. Wang, A.G. Rozhin, I.H. White, and A.C. Ferrari, Nano Res. **3**, 404 (2010).
[19] Z. Sun, A.G. Rozhin, F. Wang, V. Scardaci, W.I. Milne, I.H. White, F. Hennrich, and A.C. Ferrari, Appl. Phys. Lett. **93**, 061114 (2008).
[20] G. Della Valle, R. Osellame, G. Galzerano, N. Chiodo, G. Cerullo, P. Laporta, O. Svelto, U. Morgner, A.G. Rozhin, V. Scardaci, and A.C. Ferrari, Appl. Phys. Lett. **89**, 231115 (2006).
[21] V. Scardaci, Z.P. Sun, F. Wang, A.G. Rozhin, T. Hasan, F. Hennrich, I.H. White, W.I. Milne, and A.C. Ferrari, Adv. Mater. **20**, 4040 (2008).
[22] M.A. Solodyankin, E.D. Obraztsova, A.S. Lobach, A.I. Chernov, A.V. Tausenev, V.I. Konov, and E.M. Dianov, Opt. Lett. **33**, 1336 (2008).

[23] E.J.R. Kelleher, J.C. Travers, Z. Sun, A.G. Rozhin, A.C. Ferrari, S.V. Popov, and J.R. Taylor, Appl. Phys. Lett. **95**, 111108 (2009).
[24] A. Martinez, K. Zhou, I. Bennion, and S. Yamashita, Opt. Express **18**, 11008 (2010).
[25] Z. Sun, A.G. Rozhin, F. Wang, T. Hasan, D. Popa, W. O'Neill, and A.C. Ferrari, Appl. Phys. Lett. **95**, 253102 (2009).
[26] Z.P. Sun, T. Hasan, F. Torrisi, D. Popa, G. Privitera, F.Q. Wang, F. Bonaccorso, D.M. Basko, and A.C. Ferrari, ACS Nano **4**, 803 (2010).
[27] F. Bonaccorso, Z. Sun, T. Hasan, and A.C. Ferrari, arXiv:1006.4854v1, (2010).
[28] Z. Sun, D. Popa, T. Hasan, F. Torrisi, F. Wang, E.J.R. Kelleher, J.C. Travers, and A.C. Ferrari, arXiv:1003.4714v1, (2010).
[29] E.J.R. Kelleher, J.C. Travers, E.P. Ippen, Z. Sun, A.C. Ferrari, S.V. Popov, and J.R. Taylor, Opt. Lett. **34**, 3526 (2009).
[30] M. Zhang, L.L. Chen, C. Zhou, Y. Cai, L. Ren, and Z.G. Zhang, Laser Phys. Lett. **6**, 657 (2009).
[31] J. Fekete, A. Cserteg, and R. Szipőcs, Laser Phys. Lett. **6**, 49 (2009).
[32] W.H. Renninger, A. Chong, and F.W. Wise, Opt. Lett. **33**, 3025 (2008).
[33] S. Kobtsev, S. Kukarin, S. Smirnov, S. Turitsyn, and A. Latkin, Opt. Express **17**, 20707 (2009).
[34] R.B. Weisman and S.M. Bachilo, Nano Lett. **3**, 1235 (2003).
[35] I.A. Bufetov, K.M. Golant, S.V. Firstov, A.V. Kholodkov, A.V. Shubin, and E.M. Dianov, Appl. Opt. **47**, 4940 (2008).
[36] Y.-S. Seo, C.-H. Lim, Y. Fujimoto, and M. Nakatsuka, J. Opt. Soc. Korea **11**, 63 (2007).
[37] D.-P. Zhou, L. Wei, B. Dong, and W.-K. Liu, IEEE Photon. Technol. Lett. **22**, 9 (2010).